Contribution from the Department of Chemistry,
University of California, Davis, California 95616

Structural Changes Accompanying Oxidative Additions of Tetrachloro-1,2-benzoquinone to Phosphine-Bridged Binuclear and Trinuclear Rhodium Complexes

Alan L. Balch,* Vincent J. Catalano, and Marilyn M. Olmstead

Received September 6, 1989

Addition of tetrachloro-1,2-benzoquinone to bi- and trinuclear rhodium complexes results in conversion of terminal carbon monoxide ligands to bridging ones and the formation of new Rh–Rh bonds. These structural changes are not seen in analogous reactions of mononuclear complexes. Reaction of tetrachloro-1,2-benzoquinone with $Rh_2(CO)_2(\mu\text{-}S)(\mu\text{-dpm})_2$ (**1**) (dpm = bis(diphenylphosphino)methane) yields brown $Rh_2(1,2\text{-}O_2C_6Cl_4)(\mu\text{-}CO)(CO)(\mu\text{-}S)(\mu\text{-dpm})_2$ (**2**), which crystallizes in the monoclinic space group $P2_1/c$ as a mono(diethyl ether) solvate with a = 15.956 (3) Å, b = 21.101 (5) Å, c = 18.743 (4) Å, β = 112.14 (2)°, and Z = 4 at 130 K. Refinement of 7435 reflections with 360 parameters yielded R = 0.0560 and R_w = 0.0690. The *o*-quinone has added to one rhodium to form a chelating catecholato ligand. One of the terminal carbon monoxide ligands in **1** has been converted into a bridging ligand in **2**, and the Rh···Rh distance has shortened from 3.154 (2) Å in **1** to 2.966 (1) Å in **2**. Tetrachloro-1,2-benzoquinone also adds to the A-frame $[Rh_2(CO)_2(\mu\text{-Cl})(\mu\text{-dpm})_2][BPh_4]$ in a similar fashion to yield green $[Rh_2(1,2\text{-}O_2C_6Cl_4)(\mu\text{-CO})(CO)(\mu\text{-dpm})_2][BPh_4]$. With $[Rh_3(CO)_3(\mu\text{-Cl})(Cl)\{\mu\text{-}(Ph_2PCH_2)_2EPh\}_2][BPh_4]$ (E = P or As), the adducts $[Rh_3(1,2\text{-}O_2C_6Cl_4)(\mu\text{-CO})_2(CO)(\mu\text{-Cl})Cl\{\mu\text{-}(Ph_2PCH_2)_2EPh\}_2][BPh_4]$ are formed, in which two terminal carbonyl groups have been converted to bridging groups. These adducts can lose the dioxolene ligand, and its transfer to $Ir(CO)Cl(PH_3)_2$ has been observed.

Introduction

The reactivity patterns for mononuclear transition-metal complexes have become well understood through decades of investigation.[1] Polynuclear complexes built up from mononuclear units put in close proximity may be expected to deviate from those mononuclear components because of the enroachment of the metal centers and their associated ligands upon one another.[2] This article concerns the oxidative addition of a strongly oxidizing *o*-quinone, tetrachloro-1,2-benzoquinone, to a series of rhodium complexes.

Addition of tetrachloro-1,2-benzoquinone to various low-valent, mononuclear metal complexes results in the cis addition of two oxygen donors to form a dioxolene ligand.[3-6] In the present context, the reaction of $Rh(CO)Cl(PPh_3)_2$, shown in eq 1, is

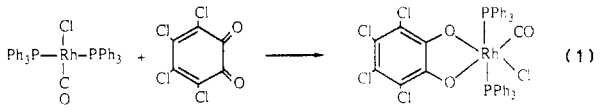

(1)

relevant.[3,4] The reaction results in conversion of the four-coordinate starting material into a six-coordinate product with folding of the CO and Cl ligands toward each other. In a polynuclear complex composed of planar, four-coordinate Rh^I units, this motion will result in crowding of the ligands and rhodium ions and may cause geometric changes at several sites within the complex. Here, this is examined in a related set of bi- and trinuclear rhodium complexes bridged by bis(diphenylphosphino)methane (dpm), bis((diphenylphosphino)methyl)phenylphosphine (dpmp), or bis((diphenylphosphino)methyl)phenylarsine (dpma). We show that the oxidative addition is accompanied by conversion of a terminal carbon monoxide ligand into a bridging ligand and formation of a Rh–Rh bond. These are features not seen in the reactions of corresponding mononuclear complexes; that is they do not associate to form metal–metal-bonded species upon oxidation.

Results and Discussion

Tetrachloro-1,2-benzoquinone Addition to $Rh_2(CO)_2(\mu\text{-}S)(\mu\text{-dpm})_2$ (1). The addition proceeds in dichloromethane according to eq 2. The product **2** is coordinately saturated at both rhodium

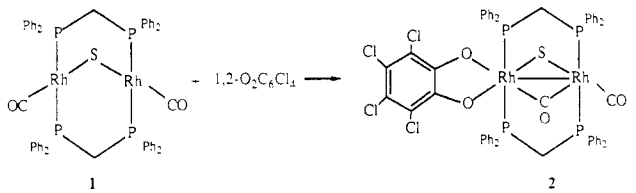

1 2

(2)

ions and is unreactive toward an excess of tetrachloro-1,2-benzoquinone. It is isolated as red-brown crystals upon addition of methanol. The infrared spectrum of **2** shows absorptions at 2000 and 1811 cm^{-1} due to a terminal and a bridging carbon monoxide ligand. The increase in ν(CO) from the values of 1920 and 1933 cm^{-1} in **1**[7] to 2000 cm^{-1} for the terminal carbonyl in **2** is consistent with an oxidation reaction. However, the terminal carbonyl group is not on the rhodium center that has been attacked by the tetrachloro-1,2-benzoquinone. Thus, although the adduct **2** could be formulated as a mixed-valence Rh^{III}–Rh^I species, the effect of oxidation is manifested throughout the molecule, in accord with Pauling's electroneutrality principle. The infrared spectrum of **2** also contains new absorptions not present in **1**, at 1520 w, 1256 s, 964 s, 800 m, and 775 cm cm^{-1} that are indicative of the presence of the dioxolene ligand.[4] The $^{31}P\{^1H\}$ NMR spectrum of **2** is of the deceptively simple variety with two doublets of apparent triplets (δ_1 = 20.9 ppm, J(Rh,P) = 124.5 Hz; δ_2 = 12.2 ppm, J(Rh,P) = 99 Hz, apparent J(P,P) = 21 Hz.) This spectrum is consistent with the structure that requires two different phosphorus environments.

X-ray Crystal Structure of $Rh_2(1,2\text{-}O_2C_6Cl_4)(\mu\text{-CO})(CO)(\mu\text{-S})(\mu\text{-dpm})_2\cdot(C_2H_5)_2O$. The material crystallizes with one molecule of **2** and one of ethyl ether in the asymmetric unit. The complex has no crystallographically imposed symmetry. A drawing of it is shown in Figure 1. Atomic coordinates are given in Table I. Table II contains selected interatomic distances and angles. Figure 2 shows a drawing of the planar section containing the dioxolene ligand, the two rhodium ions, the carbonyl groups, and the sulfide alongside a drawing of a similar plane for **1**.[7] As is readily apparent, the dioxolene ligand has bonded to Rh(1), and one of the carbonyl groups of **1** has moved to a bridging position in **2**. This clearly shows that binding a quinone to **1** results in changes at both rhodium centers because of the required motion of the carbonyl on Rh(1).

The Rh–Rh distance in **2** (2.964 (1) Å) is appreciably shorter than it is in **1** (3.154 (2) Å).[7] However, it is noticeably longer

(1) Collman, J. P.; Hegedus, L. S.; Norton, J. R.; Finke, R. G. *Principles and Applications of Organotransition Metal Chemistry*; University Science Books: Mill Valley, CA, 1987. Crabtree, R. H. *The Organometallic Chemistry of Transition Metals*; John Wiley: New York, 1988.
(2) Balch, A. L. In *Homogeneous Catalysis with Metal Phosphine Complexes*; Pignolet, L. H., Ed.; Plenum Press: New York, 1983; p 167.
(3) Sohn, Y. S.; Balch, A. L. *J. Am. Chem. Soc.* **1971**, *93*, 1296.
(4) Sohn, Y. S.; Balch, A. L. *J. Am. Chem. Soc.* **1972**, *94*, 1144.
(5) Girgis, A. Y.; Sohn, Y. S.; Balch, A. L. *Inorg. Chem.* **1975**, *14*, 2327.
(6) Pierpont, C. G.; Buchanan, R. M. *Coord. Chem. Rev.* **1981**, *38*, 45.
(7) Kubiak, C. P.; Eisenberg, R. *Inorg. Chem.* **1980**, *19*, 2726. Kubiak, C. P.; Eisenberg, R. *J. Am. Chem. Soc.* **1977**, *99*, 6129.

0020-1669/90/1329-1638$02.50/0

Table I. Atomic Coordinates (×10⁴) and Equivalent Isotropic Displacement Coefficients (Å² × 10³) for $Rh_2(1,2\text{-}O_2C_6Cl_4)(\mu\text{-}CO)(CO)(\mu\text{-}S)(\mu\text{-}dpm)_2\cdot(C_2H_5)_2O$

	x	y	z	U(eq)[a]		x	y	z	U(eq)[a]
Rh(1)	7355 (1)	162 (1)	7271 (1)	10 (1)	C(25)	6689 (6)	2518 (4)	9923 (5)	31 (2)
Rh(2)	7945 (1)	1505 (1)	7511 (1)	11 (1)	C(26)	7214 (6)	2019 (4)	9865 (5)	37 (2)
Cl(1)	7574 (1)	−1850 (1)	8763 (1)	26 (1)	C(27)	7170 (5)	1820 (4)	9142 (4)	26 (2)
Cl(2)	6661 (1)	−3006 (1)	7687 (1)	27 (1)	C(28)	8612 (5)	−777 (3)	6464 (4)	15 (2)
Cl(3)	5855 (1)	−2810 (1)	5882 (1)	27 (1)	C(29)	8978 (5)	−1368 (4)	6718 (5)	25 (2)
Cl(4)	5784 (1)	−1439 (1)	5208 (1)	27 (1)	C(30)	8870 (6)	−1859 (4)	6206 (5)	33 (2)
S	7103 (1)	996 (1)	6347 (1)	14 (1)	C(31)	8363 (6)	−1769 (4)	5436 (5)	32 (2)
P(1)	5999 (1)	449 (1)	7418 (1)	11 (1)	C(32)	7989 (6)	−1185 (4)	5171 (5)	31 (2)
P(2)	6569 (1)	1861 (1)	7532 (1)	13 (1)	C(33)	8101 (5)	−687 (4)	5687 (4)	23 (2)
P(3)	8713 (1)	−127 (1)	7131 (1)	12 (1)	C(34)	9685 (5)	−321 (3)	8008 (4)	12 (1)
P(4)	9186 (1)	1287 (1)	7185 (1)	12 (1)	C(35)	10565 (5)	−318 (3)	8008 (4)	19 (2)
O(1)	9001 (4)	2448 (3)	8720 (3)	38 (2)	C(36)	11292 (6)	−415 (4)	8684 (4)	26 (2)
O(2)	8375 (3)	649 (2)	8834 (3)	16 (1)	C(37)	11175 (5)	−505 (3)	9377 (4)	20 (2)
O(3)	7495 (3)	−662 (2)	7930 (3)	13 (1)	C(38)	10323 (5)	−520 (3)	9377 (4)	18 (2)
O(4)	6661 (3)	−465 (2)	6391 (3)	13 (1)	C(39)	9561 (5)	−441 (3)	8693 (4)	15 (2)
C(1)	8600 (5)	2059 (3)	8292 (4)	18 (2)	C(40)	9146 (5)	521 (3)	6717 (4)	12 (1)
C(2)	8031 (5)	693 (3)	8171 (4)	13 (1)	C(41)	10294 (5)	1327 (3)	7983 (4)	16 (2)
C(3)	5984 (5)	373 (3)	8384 (4)	15 (1)	C(42)	11060 (5)	1522 (3)	7859 (4)	22 (2)
C(4)	6557 (5)	−65 (3)	8891 (4)	16 (2)	C(43)	11877 (6)	1589 (4)	8481 (5)	31 (2)
C(5)	6564 (5)	−126 (3)	9637 (4)	19 (2)	C(44)	11943 (6)	1461 (4)	9214 (5)	26 (2)
C(6)	6009 (5)	246 (4)	9868 (5)	26 (2)	C(45)	11193 (5)	1251 (4)	9345 (4)	23 (2)
C(7)	5439 (6)	673 (4)	9370 (5)	33 (2)	C(46)	10377 (5)	1190 (3)	8732 (4)	20 (2)
C(8)	5429 (6)	740 (4)	8633 (5)	27 (2)	C(47)	9345 (5)	1855 (3)	6516 (4)	17 (2)
C(9)	5023 (5)	21 (3)	6795 (4)	15 (2)	C(48)	9341 (5)	2495 (3)	6691 (4)	20 (2)
C(10)	4531 (5)	−390 (3)	7066 (4)	21 (2)	C(49)	9567 (5)	2941 (4)	6262 (4)	27 (2)
C(11)	3778 (6)	−699 (4)	6547 (5)	28 (2)	C(50)	9804 (6)	2760 (4)	5653 (5)	28 (2)
C(12)	3509 (6)	−602 (4)	5762 (5)	30 (2)	C(51)	9792 (6)	2127 (4)	5468 (5)	33 (2)
C(13)	4000 (5)	−203 (3)	5486 (4)	21 (2)	C(52)	9568 (5)	1674 (4)	5895 (4)	28 (2)
C(14)	4759 (5)	107 (3)	5997 (4)	20 (2)	C(53)	7093 (5)	−1147 (3)	7479 (4)	13 (1)
C(15)	5668 (5)	1272 (3)	7143 (4)	14 (1)	C(54)	7068 (5)	−1747 (3)	7772 (4)	15 (2)
C(16)	6114 (5)	2558 (3)	6939 (4)	17 (2)	C(55)	6672 (5)	−2262 (3)	7296 (4)	19 (2)
C(17)	5196 (6)	2652 (4)	6550 (5)	33 (2)	C(56)	6301 (5)	−2170 (3)	6505 (4)	18 (2)
C(18)	4883 (6)	3234 (4)	6188 (5)	30 (2)	C(57)	6289 (5)	−1563 (3)	6194 (4)	16 (2)
C(19)	5462 (5)	3696 (4)	6190 (4)	25 (2)	C(58)	6659 (5)	−1048 (3)	6663 (4)	15 (2)
C(20)	6387 (6)	3601 (4)	6547 (5)	34 (2)	O(5)	1848 (7)	5109 (4)	1887 (6)	88 (3)
C(21)	6711 (6)	3034 (4)	6917 (4)	27 (2)	C(59)[b]	630	5618	842	90
C(22)	6588 (5)	2118 (3)	8475 (4)	17 (2)	C(60)	1291 (10)	5125 (7)	1111 (8)	91 (5)
C(23)	6045 (5)	2606 (4)	8542 (4)	25 (2)	C(61)	2373 (7)	4573 (5)	2092 (6)	55 (3)
C(24)	6110 (6)	2814 (4)	9266 (5)	31 (2)	C(62)	2980 (8)	4598 (6)	2912 (7)	73 (4)

[a] Equivalent isotropic U defined as one-third of the trace of the orthogonalized U_{ij} tensor. [b] Positional and thermal parameters of C(59), the methyl carbon of a diethyl ether molecule, were fixed due to poor convergence.

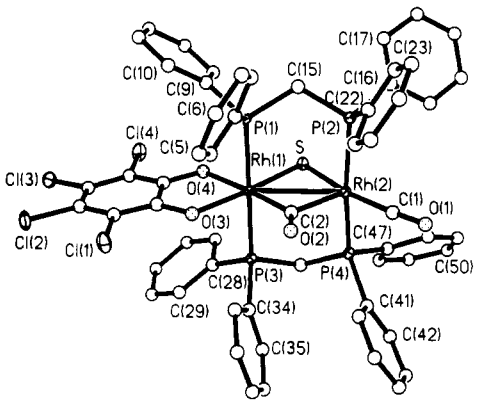

Figure 1. Perspective view of $Rh_2(1,2\text{-}O_2C_6Cl_4)(\mu\text{-}CO)(CO)(\mu\text{-}S)(\mu\text{-}dpm)_2$ (**2**), showing 50% thermal contours for Rh, P, S, and Cl and uniform, arbitarily sized circles for carbon and oxygen.

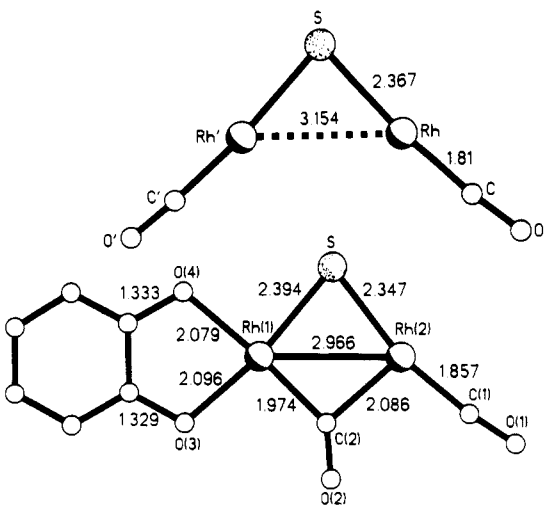

Figure 2. Comparison of the core structures of $Rh_2(CO)_2(\mu\text{-}S)(\mu\text{-}dpm)_2$ (top) and $Rh_2(1,2\text{-}O_2C_6Cl_4)(\mu\text{-}CO)(CO)(\mu\text{-}S)(\mu\text{-}dpm)_2$ (bottom).

than the range (2.72–2.89 Å) of Rh–Rh or Ir–Ir distances seen for other related carbonyl-bridged units in which there is a metal–metal bond.[8,9] On the other hand, it is considerably shorter than the range (3.35–3.41 Å) found[10] for the so-called ketonic carbonyls, where the Rh···Rh separation precludes any direct metal–metal bond. As Figure 2 shows, the bridging groups in

(8) Sutherland, B. R.; Cowie, M. *Inorg. Chem.* **1984**, *23*, 2324. Gelmini, L.; Stephan, D. W.; Loeb, S. J. *Inorg. Chim. Acta* **1985**, *98*, L3. Cowie, M.; Dwight, S. K. *Inorg. Chem.* **1980**, *19*, 2508. Sutherland, B. R.; Cowie, M. *Inorg. Chem.* **1984**, *23*, 2324. Balch, A. L.; Fossett, L. A.; Guimerans, R. R.; Olmstead, M. M.; Reedy, P. E., Jr. *Inorg. Chem.* **1986**, *25*, 1397. Olmstead, M. M.; Guimerans, R. R.; Balch, A. L. *Inorg. Chem.* **1983**, *22*, 2473. Balch, A. L.; Olmstead, M. M.; Guimerans, R. R. *Inorg. Chim. Acta* **1984**, *84*, L21. Balch, A. L.; Fossett, L. A.; Olmstead, M. M.; Reedy, P. E., Jr. *Organometallics* **1988**, *7*, 430.

(9) Kubiak, C. P.; Woodcock, C.; Eisenberg, R. *Inorg. Chem.* **1980**, *19*, 2733.

(10) Cowie, M.; Southern, T. G. *Inorg. Chem.* **1982**, *21*, 246. Mague, J. T. *Inorg. Chem.* **1983**, *22*, 45. Balch, A. L.; Fossett, L. A.; Linehan, J.; Olmstead, M. M. *Organometallics* **1986**, *5*, 691.

Table II. Selected Interatomic Distances and Angles for $Rh_2(1,2\text{-}O_2C_6Cl_4)(\mu\text{-}CO)(CO)(\mu\text{-}S)(\mu\text{-}dpm)_2\cdot(C_2H_5)_2O$

	Distances (Å)		
	At Rh(1)		
Rh(1)–Rh(2)	2.966 (1)	Rh(1)–P(1)	2.360 (2)
Rh(1)–S	2.394 (2)	Rh(1)–P(2)	2.359 (2)
Rh(1)–C(3)	2.096 (5)	Rh(1)–O(4)	2.079 (4)
Rh(1)–C(2)	1.974 (6)		
	At Rh(2)		
Rh(2)–C(1)	1.857 (7)	Rh(2)–C(2)	2.086 (7)
Rh(2)–P(2)	2.336 (2)	Rh(2)–P(4)	2.328 (2)
Rh(2)–S	2.347 (2)		
	For the Catecholato Ligand		
C(53)–O(3)	1.329 (8)	C(58)–O(4)	1.333 (8)
C(53)–C(54)	1.388 (10)	C(56)–C(57)	1.404 (10)
C(54)–C(55)	1.396 (9)	C(57)–C(58)	1.381 (9)
C(55)–C(56)	1.388 (10)	C(58)–C(53)	1.437 (9)
Cl(1)–C(54)	1.738 (7)	Cl(3)–C(56)	1.752 (7)
Cl(2)–C(55)	1.736 (8)	Cl(4)–C(57)	1.735 (7)
	Angles (deg)		
	At Rh(1)		
P(1)–Rh(1)–P(3)	179.7 (1)	O(4)–Rh(1)–C(2)	174.9 (2)
S–Rh(1)–O(3)	171.0 (1)		
S–Rh(1)–C(2)	95.1 (2)	O(3)–Rh(1)–C(2)	93.7 (2)
S–Rh(1)–P(1)	89.0 (1)		
S–Rh(1)–P(3)	91.2 (1)		
S–Rh(1)–O(4)	90.0 (4)	O(3)–Rh(1)–O(4)	81.2 (2)
P(1)–Rh(1)–O(3)	92.5 (2)	Rh(2)–Rh(1)–O(3)	138.3 (1)
P(1)–Rh(1)–O(4)	91.0 (2)	Rh(2)–Rh(1)–S	50.6 (1)
P(1)–Rh(1)–C(2)	89.1 (2)	Rh(2)–Rh(1)–C(2)	44.6 (2)
P(3)–Rh(1)–C(2)	90.7 (2)	Rh(2)–Rh(1)–P(1)	89.4 (1)
P(3)–Rh(1)–O(3)	87.3 (2)	Rh(2)–Rh(1)–P(3)	90.7 (1)
P(3)–Rh(1)–O(4)	89.1 (2)		
	At Rh(2)		
P(2)–Rh(2)–P(4)	165.0 (1)	Rh(1)–Rh(2)–C(1)	140.7 (2)
S–Rh(2)–C(1)	167.3 (2)	Rh(1)–Rh(2)–P(2)	93.6 (1)
S–Rh(2)–C(2)	93.6 (2)	Rh(1)–Rh(2)–P(4)	91.4 (1)
S–Rh(2)–P(2)	87.1 (1)	Rh(1)–Rh(2)–C(2)	41.6 (2)
S–Rh(2)–P(4)	84.9 (1)	Rh(1)–Rh(2)–S	52.0 (1)
P(2)–Rh(2)–C(1)	92.2 (3)	C(1)–Rh(2)–C(2)	99.1 (3)
P(2)–Rh(2)–C(2)	96.1 (2)		
P(4)–Rh(2)–C(1)	92.9 (3)		
P(4)–Rh(2)–C(2)	97.0 (2)		
	At S		
Rh(1)–S–Rh(2)	77.5 (1)		
	At C(2)		
Rh(1)–C(2)–O(2)	139.1 (5)	Rh(2)–C(2)–O(2)	127.0 (5)
Rh(1)–C(2)–Rh(2)	93.8 (3)		
	For the Catecholato Ligand		
O(3)–C(53)–C(58)	119.3 (6)	O(3)–C(53)–C(54)	122.0 (6)
Cl(1)–C(54)–C(53)	117.8 (5)	C(54)–C(53)–C(58)	118.7 (6)
C(53)–C(54)–C(55)	122.0 (6)	Cl(1)–C(54)–C(55)	120.1 (5)
Cl(2)–C(55)–C(56)	120.6 (5)	Cl(2)–C(55)–C(54)	120.6 (5)
Cl(3)–C(56)–C(55)	120.5 (6)	C(54)–C(55)–C(56)	118.8 (7)
C(55)–C(56)–C(57)	120.3 (6)	Cl(3)–C(56)–C(57)	119.2 (5)
Cl(4)–C(57)–C(58)	118.3 (5)	Cl(4)–C(57)–C(56)	120.5 (5)
O(4)–C(58)–C(53)	118.1 (6)	C(56)–C(57)–C(58)	121.2 (6)
C(53)–C(58)–C(57)	118.8 (6)	O(4)–C(58)–C(57)	123.0 (6)

2 are more unsymmetrically positioned than they are in the A-frame **1**. The double A-frame, $[Ir_2(\mu\text{-}CO)(CO)_2(\mu\text{-}S)(\mu\text{-}dpm)_2]$, also has a symmetric structure with an Ir–S bond length of 2.463 (3) Å, an Ir–C bond length of 1.80 (1) Å, and an Ir–Ir bond length of 2.843 (2) Å. Thus, the Rh(1)–S distance (2.394 (2) Å) is longer than the Rh(2)–S distance (2.347 (2) Å), and the Rh(1)–C(2) distance (1.974 (6) Å) is shorter than the Rh(2)–C(2) distance (2.086 (7) Å). This asymmetry is caused by the bonding of the added catecholato ligand to one rhodium, which makes each rhodium unique.

The dimensions of the dioxolene ligand clearly indicate that the catecholato oxidation state (rather than the semiquinone or quinone state) is the major contributor to the ground-state structure. Thus the C–O bond lengths (1.329 (8), 1.333 (8) Å) are longer than the C=O bond length in tetrachloro-*p*-quinone (1.20 (1) Å)[11] and comparable to those in tetrachloro-1,2-hydroquinone (1.35 (1) Å).[12] The C=C bond lengths within this ligand are nearly equal. The bond length alternation expected for a quinone oxidation state is absent. The structural parameters of this moiety are similar to those found in other complexes formulated as containing *o*-catecholato ligands including $(Ph_3P)_2Pd(1,2\text{-}O_2C_6Cl_4)$,[13] $(Ph_3P)Ir(NO)(1,2\text{-}O_2C_6Cl_4)$,[14] and $Rh_2(1,2\text{-}O_2C_6Cl_4)(CO)(\mu\text{-}dpm)_2$.[15] However, the Rh—O bond lengths in **2** (2.096 (5), 2.079 (4) Å) are significantly longer than the range (1.905–2.052 Å) seen for these other catecholato complexes.

Tetrachloro-1,2-benzoquinone Addition to $[Rh_2(CO)_2(\mu\text{-}Cl)(\mu\text{-}dpm)_2][BPh_4]$ (3).[16-18] In dichloromethane, yellow **3** is converted into green **4** upon addition of tetrachloro-1,2-benzoquinone (eq 3) in a reaction that parallels that of the sulfur-bridged A-frame

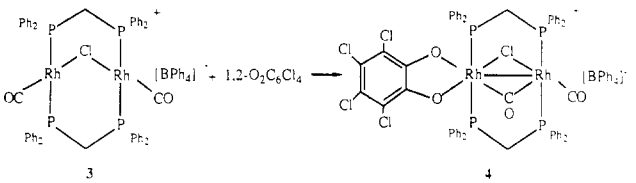

(3)

1. The infrared spectrum shows carbon monoxide stretching vibrations at 2042 and 1865 cm^{-1} and bands characteristic of the coordinated catecholato ligand at 1510 vw, 1257 s, 969 s, 813 m, and 797 m cm^{-1}. The carbonyl absorptions are consistent with the presence of a terminal and a bridging carbon monoxide ligand. These occur at higher energies in **4** relative to **2** because of the positive charge on the complex in the former. The increase in the terminal carbonyl stretching frequency from 1976 cm^{-1} in **3** (or 1980 cm^{-1} for $[Rh_2(\mu\text{-}CO)(CO)_2(\mu\text{-}Cl)(\mu\text{-}dpm)_2]^+$) to 2042 cm^{-1} in **4** is indicative of an oxidative process. As with **2**, it is the carbonyl group bound to the rhodium that is removed from the catecholato ligand that shows the increase in $\nu(C{\equiv}O)$. Again, this shows the effect of the overall distribution of the electron withdrawal by the added ligand. The $^{31}P\{^1H\}$ NMR spectrum consists of two triplets of doublets with δ_1 = 9.9 ppm (J(Rh,P) = 89.8 Hz) and δ_2 = 22.6 ppm (J(Rh,P) = 94 Hz, apparent J(P,P) = 24.4 Hz). The decrease in J(Rh,P) seen at both rhodium ions in **4** relative to the 113.7-Hz coupling seen in **3** is indicative of the oxidation affecting both rhodium centers.

Addition of Tetrachloro-1,2-benzoquinone to Trirhodium Complexes. Addition of the quinone to $[Rh_3(CO)_3(\mu\text{-}Cl)Cl(\mu\text{-}dpmp)_2][BPh_4]$ (**5**)[19] and $[Rh_3(CO)_3(\mu\text{-}Cl)Cl(\mu\text{-}dpma)_2][BPh_4]$ (**7**)[19] proceeds as shown in eq 4 to form analogous adducts $[Rh_3(1,2\text{-}O_2C_6Cl_4)(\mu\text{-}CO)_2(CO)(\mu\text{-}Cl)Cl(\mu\text{-}dpmp)_2][BPh_4]$ (**6**) and $[Rh_3(1,2\text{-}O_2C_6Cl_4)(\mu\text{-}CO)_2(CO)(\mu\text{-}Cl)Cl(\mu\text{-}dpma)_2][BPh_4]$ (**8**). The infrared spectra of the adducts clearly reveal that two of the terminal carbonyl groups in **5** and **7** have been converted into bridging groups in the adducts. These spectra are similar for **6** and **8**. For **6** the relevant absorptions (Nujol mull) are 2034 s, 1986 sh, 1833 s, and 1796 s cm^{-1}, while for **8** they are 2029 s, 1985 m, 1836 s, and 1769 cm^{-1}. The bands at 1986 (**6**) and 1985 (**8**) cm^{-1} are believed to be overtones or combination bands

(11) Chu, S. S. C.; Jeffrey, G. A.; Sakurai, T. *Acta Crystallogr.* **1962**, *15*, 661.
(12) Sikka, S. K.; Chidambaran, R. *Acta Crystallogr.* **1967**, *23*, 107.
(13) Pierpont, C. G.; Downs, H. H. *Inorg. Chem.* **1975**, *14*, 343.
(14) Shorthill, W. B.; Buchanan, R. M.; Pierpont, C. G.; Ghedini, M.; Dolcetti, G. *Inorg. Chem.* **1980**, *19*, 1803.
(15) Ladd, J. A.; Olmstead, M. M.; Balch, A. L. *Inorg. Chem.* **1984**, *23*, 2318.
(16) Olmstead, M. M.; Lindsay, C. H.; Benner, L. S.; Balch, A. L. *J. Organomet. Chem.* **1979**, *179*, 289.
(17) Mague, J. T.; Sanger, A. R. *Inorg. Chem.* **1979**, *18*, 2060.
(18) Cowie, M.; Dwight, S. K. *Inorg. Chem.* **1979**, *18*, 2700.
(19) Balch, A. L.; Fosett, L. A.; Guimerans, R. R.; Olmstead, M. M.; Reedy, P. E., Jr.; Wood, F. E. *Inorg. Chem.* **1986**, *25*, 1248.
(20) Balch, A. L.; Fossett, L. A.; Olmstead, M. M.; Reedy, P. E., Jr. *Organometallics* **1986**, *5*, 1929.

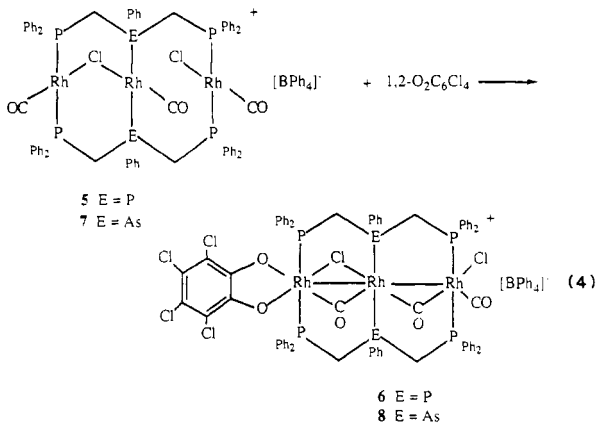

5 E = P
7 E = As

6 E = P
8 E = As

(from the 1000–900-cm^{-1} region) that steal intensity from the strong terminal carbonyl absorption at 2034 or 2029 cm^{-1}. For the adduct, the infrared bands characteristic of the catecholato ligands are seen at 1520 w, 1255 s, 999 s, 806 m and 780 sh cm^{-1} for **6** and at 1253 s, 999 s, 805 m, and 790 cm^{-1} for **8**.

The $^{31}P\{^1H\}$ NMR spectrum of **6** is entirely consistent with a structure involving three distinct types of phosphorus atoms. It is reproduced in Figure 3 and gives the values δ_1 = 6.9 ppm (J(Rh,P) = 95.4 Hz, apparent J(P,P) = 20 Hz), δ_2 = 11.6 (J(Rh,P) = 108 Hz), and δ_3 = 28.1 ppm (J(Rh,P) = 110 Hz, apparent J(P,P) = 31 Hz). The complex multiplet centered at 11.6 ppm is assigned to the internal phosphorus atom in a dpmp ligand, while the other, simpler patterns are due to each of the two end environments. Smaller peaks centered at 23 and 15.5 ppm result from small amounts of the starting complex [Rh_3-$(CO)_3(\mu$-Cl)Cl(μ-dpmp)$_2$][BPh_4] that form as a result of quinone dissociation (vide infra). The $^{31}P\{^1H\}$ NMR spectrum of **8** is much less complex, since the two end phosphorus environments are no longer coupled to a central phosphorus. The spectrum in dichloromethane consists of two doublets at δ = 28.4 ppm (^1J(Rh,P) = 116.8 Hz) and δ = 7.1 ppm (^1J(Rh,P) = 94.4 Hz). Again, dissociation of the quinone occurs since a doublet at 24.3 ppm (^1J(Rh,P) = 118.8 Hz) due to **7** is present. Addition of further tetrachloro-1,2-benzoquinone results in the loss of the doublet due to **7** and an increase in the intensity of the peaks due to **8**.

As expected for **6**, the ^1H NMR spectrum in chloroform-*d* solution shows four methylene resonances at 4.60, 4.25, 3.50, and 3.05 ppm, which exhibit complex splitting due to coupling to phosphorus and to the other geminal proton. A complex phenyl resonance pattern is seen in the 6.7–7.7 ppm region. Similarly, **8** shows methylene resonances at 4.42, 4.08, 3.39, and 2.90 ppm and a phenyl multiplet in the region 6.6–7.8 ppm.

Tetrachloro-1,2-benzoquinone-Transfer Reactions. Earlier we had noted that recrystallization of Rh(1,2-$O_2C_6Cl_4$)(CO)(PPh_3)$_2$ resulted in loss of the dioxolene ligand and recovery of Rh-(CO)Cl(PPh_3)$_2$.[4] Since the ^{31}P NMR spectra of some of the benzoquinone adducts give evidence of dissociation of the benzoquinone from the complex, experiments designed to detect transfer of the dioxolene ligand from one complex to another were undertaken. We utilized Ir(CO)Cl(PPh_3)$_2$ for this, since it readily forms an adduct with tetrachloro-1,2-benzoquinone,[3,4] and the Ir–O bonds of this adduct may be expected to be considerably stronger than the Rh–O bonds of the polynuclear complexes described here.

Figure 4 shows the $^{31}P\{^1H\}$ NMR spectrum obtained from a mixture of [Rh_2(1,2-$O_2C_6Cl_4$)(μ-CO)(CO)(μ-Cl)(μ-dpm)$_2$][BPh_4] (**4**) and Ir(CO)Cl(PPh_3)$_2$ in chloroform. The top spectrum shows the sample immediately after preparation. The singlet of the iridium complex and the two doublets of triplets of **4** are apparent along with the singlet of Ir(O_2)(CO)Cl(PPh_3)$_2$, which forms due to leakage of dioxygen into the NMR tube. After the mixture is allowed to stand for 18 h, the spectrum shown at the bottom is obtained. All of **4** has gone, and a new resonance at −17.7 ppm (due to Ir(1,2-$O_2C_6Cl_4$)(CO)Cl(PPh_3)$_2$) and a new multiplet at 20 ppm (due to [Rh_2(CO)$_2$(μ-Cl)(dpm)$_2$][BPh_4] (**3**)) have appeared. The intensity of the peak due to the dioxygen adduct,

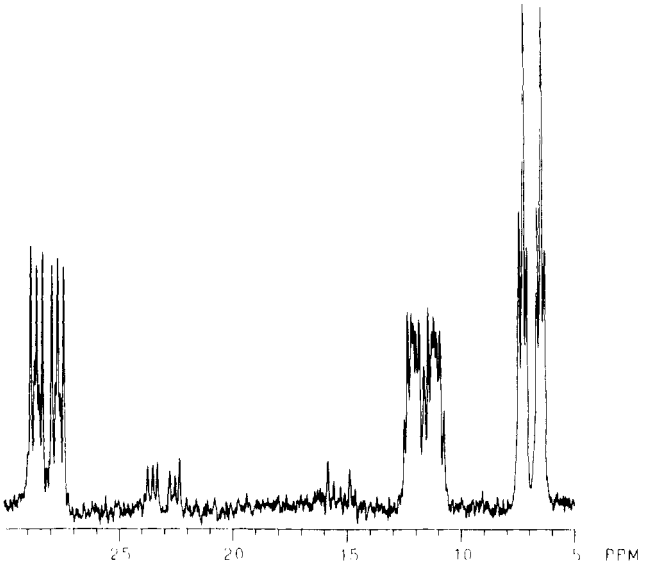

Figure 3. 121-MHz $^{31}P\{^1H\}$ NMR spectrum of [Rh_3(1,2-$O_2C_6Cl_4$)(μ-CO)$_2$(CO)(μ-Cl)Cl(μ-dpmp)$_2$][BPh_4] in dichloromethane solution at 25 °C.

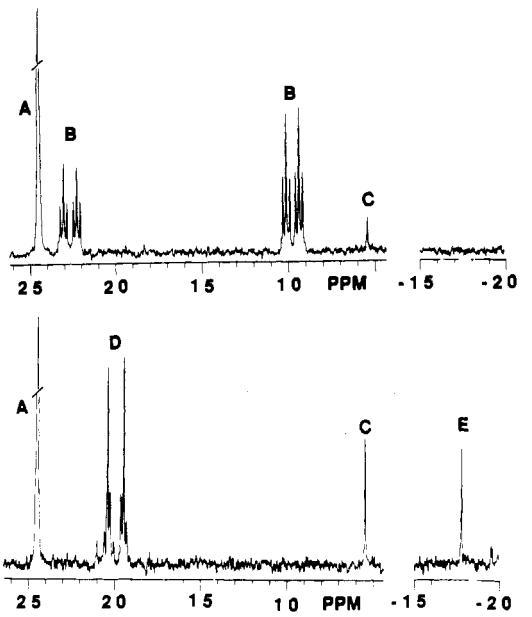

Figure 4. 121-MHz $^{31}P\{^1H\}$ NMR spectra showing the transfer of tetrachloro-1,2-benzoquinone between complexes for a mixture of Ir(CO)-Cl(PPh_3)$_2$ (peak A) and [Rh_2(1,2-$O_2C_6Cl_4$)(μ-CO)(CO)(μ-Cl)-(dpm)$_2$][BPh_4] (peak B): top, just after preparation; bottom, after 18 h. The resonance due to Ir(1,2-$O_2C_6Cl_4$)(CO)Cl(PPh_3)$_2$ is labeled E, those of [Rh_2(CO)$_2$(μ-Cl)(μ-dpm)$_2$][BPh_4] are labeled D, and that of Ir(O_2)(CO)Cl(PPh_3)$_2$ is labeled C.

Ir(O_2)(CO)Cl(PPh_3)$_2$, has also grown because of continual leakage of air into the sample. The quinone transfer is not quantitative. Although all of **3** has reacted, an insufficient quantity of Ir(1,2-$O_2C_6Cl_4$)(CO)Cl(PPh_3)$_2$ is detected in the spectrum to account for all of the tetrachloro-1,2-benzoquinone liberated. This may be due to loss of the iridium complex from solution through precipitation, establishment of an equilibrium that leaves a significant quantity of the quinone in solution, or loss of the quinone through other, undetected reactions.

A similar experiment involving [Rh_3(1,2-$O_2C_6Cl_4$)(μ-CO)$_2$-(CO)(μ-Cl)Cl(μ-dpma)$_2$][BPh_4] and Ir(CO)Cl(PPh_3)$_2$ also shows the transfer to form **7** and Ir(1,2-$O_2C_6Cl_4$)(CO)Cl(PPh_3)$_2$. Attempts to observe transfer from **6** were hampered by solubility limitations.

Experimental Section

Preparation of Compounds. $Rh_2(CO)_2(\mu$-S)(μ-dpm)$_2$,[7] [Rh_2(CO)$_2$-(μ-Cl)(μ-dpm)$_2$][BPh_4],[17] [$Rh_3(CO)_3(\mu$-Cl)Cl(μ-dpmp)$_2$][BPh_4],[19] and

Table III. Crystal Data

empirical formula	$C_{62}H_{54}O_5P_4Cl_4Rh_2S$	V	5845 (2) Å^3
		Z	4
fw	1382.6	T	130 K
color; habit	red-brown; rhombus	D_{calc}	1.571 g/cm^3
		abs coeff	0.930 mm^{-1}
cryst size	0.37 × 0.45 × 0.45 mm	radiation	Mo Kα (λ = 0.71073 Å)
cryst syst	monoclinic	range of transm factors	0.66–0.75
space group	$P2_1/c$		
unit cell dimens	a = 15.956 (3) Å	R^a	0.0560
	b = 21.101 (5) Å	$R_w{}^a$	0.0690
	c = 18.743 (4) Å		
	β = 112.14 (2)°		

$^a R = \sum||F_o| - |F_c||/|F_o|$ and $R_w = \sum||F_o| - |F_c||/w^{1/2}\sum|F_o w^{1/2}|$; $w^{-1} = \sigma^2(F) + 0.0012F^2$.

$[Rh_3(CO)_3(\mu\text{-Cl})Cl(\mu\text{-dpma})_2][BPh_4]$[19] were prepared by established routes. The products reported below have good stability toward oxygen and moisture, and no special precautions were taken in their synthesis.

$Rh_2(1,2\text{-}O_2C_6Cl_4)(\mu\text{-CO})(CO)(CO)(\mu\text{-S})(\mu\text{-dpm})_2$ (2). A solution of 32 mg (0.13 mmol) of tetrachloro-1,2-benzoquinone in 1 mL of dichloromethane was added to a red solution of 108 mg (0.10 mml) of $Rh_2(CO)_2(\mu\text{-S})(\mu\text{-dpm})_2$ in 6 mL of dichloromethane. The brown solution was filtered, and 20 mL of methanol was added. The mixture was stored at −10 °C for 12 h, and then the brown, crystalline product was collected by filtration. It was washed with methanol and vacuum-dried; yield 42 mg (32%). Anal. Calcd for $C_{58}H_{44}Cl_4O_4P_4Rh_2S$: C, 53.2; H, 3.4. Found: C, 52.8; H, 3.5.

$[Rh_2(1,2\text{-}O_2C_6Cl_4)(\mu\text{-CO})(CO)(\mu\text{-Cl})(\mu\text{-dpm})_2][BPh_4]$ (4). A solution of 22 mg (0.090 mmol) of tetrachloro-1,2-benzoquinone in 1 mL of dichloromethane was added dropwise to a yellow-orange solution of 102 mg (0.074 mmol) of $[Rh_2(CO)_2(\mu\text{-Cl})(\mu\text{-dpm})_2][BPh_4]$ in 5 mL of dichloromethane. The green solution was filtered, and ethyl ether was slowly added. The deep green, crystalline product was collected by filtration, washed with ethyl ether, and vacuum-dried; yield 77 mg (64%). Anal. Calcd for $C_{82}H_{64}BCl_5O_4P_4Rh_2$: C, 60.4; H, 3.9. Found: C, 59.6; H, 3.8.

$[Rh_3(1,2\text{-}O_2C_6Cl_4)(\mu\text{-CO})_2(CO)(\mu\text{-Cl})Cl(\mu\text{-dpmp})_2][BPh_4]\cdot CH_2Cl_2$ (6). A solution of 20 mg (0.081 mmol) of tetrachloro-1,2-benzoquinone in 1 mL of dichloromethane was added to a slurry of 100 mg (0.056 mmol) of $[Rh_3(CO)_3(\mu\text{-Cl})Cl(\mu\text{-dpmp})_2][BPh_4]$ in 5 mL of dichloromethane. After standing for 15 min, the intense blue violet solution was filtered, and ethyl ether was added dropwise to the filtrate. The violet crystals, which precipitated, were collected by filtration, washed with ethyl ether, and vacuum-dried; yield 79 mg (69%). Anal. Calcd for $C_{98}H_{80}BCl_8O_5P_6Rh_3$: C, 55.3; H, 3.8; Cl, 13.3. Found: C, 55.2; H, 3.7; Cl, 12.5. The presence of dichloromethane entrained in the crystal was verified by NMR spectroscopy.

$[Rh_3(1,2\text{-}O_2C_6Cl_4)(\mu\text{-CO})_2(CO)(\mu\text{-Cl})Cl(\mu\text{-dpma})_2][BPh_4]\cdot{}^1/_2CH_2Cl_2$ (8). This complex was obtained as purple crystals starting from $[Rh_3(CO)_3(\mu\text{-Cl})Cl(\mu\text{-dpma})_2][BPh_4]$ by the method outlined for the dpmp analogue above; yield 84%. Anal. Calcd for $C_{95}H_{79}As_2BCl_7O_5P_4Rh_3$: C, 53.9; H, 3.6; Cl, 11.4. Found: C, 53.9; H, 3.7; Cl, 11.0.

X-ray Crystallographic Study. Red-brown rhombohedrons of the complex $Rh_2(1,2\text{-}O_2C_6Cl_4)(\mu\text{-CO})(CO)(\mu\text{-S})(\mu\text{-dpm})_2\cdot(C_2H_5)_2O$ were obtained by diffusion of ethyl ether into a dichloromethane solution of the complex over 4 days. A suitable crystal was mounted on a glass fiber with silicone grease and positioned in the cold stream of a Siemens R3m/v diffractometer. Only random fluctuations (<2%) were observed in the intensity of two standard reflections during the course of data collection. Crystal data are given in Table III.

The usual corrections for Lorentz and polarization effects were applied to the data. Crystallographic programs used were those of SHELXTL PLUS, installed on a MicroVax II computer. Scattering factors and corrections for anomalous dispersion were from ref 21.

The structure was solved by direct methods. An absorption correction was applied.[22] Final refinement was carried out with anisotropic thermal parameters for rhodium, phosphorus, chlorine, and sulfur and isotropic parameters for carbon and oxygen. Hydrogen atoms were included at positions calculated by using a riding model with a C–H distance of 0.96 Å and a fixed isotropic $U_H = 1.2U_C$. The largest peak in the final difference map was 2.1 e Å^{-3}.

Acknowledgment. We thank the National Science Foundation (Grants CHE 8519557 and CHE 894209) for support and Johnson Matthey, Inc., for a loan of rhodium salts. The diffraction and computing equipment used in this study were purchased under NSF Grant CHE-8802721 to the University of California, Davis, CA.

Supplementary Material Available: Tables of bond distances, bond angles, anisotropic thermal parameters, hydrogen atom positions, and crystal and refinement data for **2** (6 pages); a listing of observed and calculated structure factors (37 pages). Ordering information is given on any current masthead page.

(21) *International Tables for X-ray Crystallography*; Kynoch: Birmingham, England, 1974; Vol. 14.

(22) The method obtains an empirical absorption tensor from an expression relating F_o and F_c: Moezzi, B. Ph.D. Thesis, University of California, Davis, CA, 1987.